

A 50-kW Boost Dc/dc Converter for Fuel Cell Applications

*Designed a 50-kW Boost dc/dc Converter including the controller for a Fuel Cell stack

1st Zhaofeng Tian
College of Engineering
Wayne State University
Detroit, the United States
gy8217@wayne.edu

Abstract—Fuel cells are static devices that utilize an electrochemical process to convert chemical energy of a fuel into electrical energy. However, the output voltage of a fuel cell stack is a function of its load and other operating parameters including its working temperature. Boost dc/dc converter is used to step up voltage from its supply to its load which is also widely used to modulate the output voltage of fuel cell stacks. This study is a model and instructions for a 50-kW boost DC/DC converter for fuel cell application including boost converter design and controller design. This study designed the boost converter operating in CCM (Continuous Conduction Model) including the controller to meet the output requirements of a 50-kW PEMFC stack. By designing the circuit, the controller and simulation, the boost converter including controller could product 480 V output voltage from 200 V input voltage at 50-kW rated power. Meanwhile, the input current ripple and output voltage ripple are both limited within 5%.

Index Terms—Fuel Cell Stack, Boost Converter, Controller Design

I. INTRODUCTION

Switch mode boost (step-up) DC/DC converters originated with the development of pulse width modulated (PWM) boost converters. Step-up dc–dc topologies convert lower dc voltage levels to higher levels by temporarily storing the input energy and then releasing it into the output at a higher volt- age level. Such storage can occur in either magnetic field storage components (single inductor/coupled inductor) or electric field storage components (capacitors) through the use of various active or passive switching elements (power switches and diodes) [1].

A PWM boost converter is a fundamental dc–dc voltage step- up circuit with several features that make it suitable for various applications in products ranging from low-power portable de- vices to high-power stationary applications. The widespread application of PWM boost dc–dc converters has been driven by its low number of elements, which is a major advantage in terms of simplifying modeling, design implementation, and manufacturing.

PEMFCs are dominating the automobile industry due to their low operating temperature and the quick startup [2], but

due to that Fuel cell output voltage varies as load changes, dc/dc converter of PEMFC stack is an important device for successful applications. In this study, a PMW boost converter with PI controller is designed to regulate the output of a 50-kW Proton Exchange Membrane Fuel Cell (PEMFC) stack.

II. CIRCUIT DESIGN

A. Design requirements of boost converter

The design requirements of the boost converter were shown at below in Table I.

TABLE I. BOOST CONVERTER DESIGN REQUIREMENTS

Converter Specification	Value
Input Voltage, V_i	200 V
Output Voltage, V_o	480 V
Rated power	50 kW
Input Current Ripple	$\leq 20\%$
Output Voltage Ripple	$\leq 5\%$

B. Circuit Model and Parameters Evaluation

To evaluate the value of parameters in the circuit, firstly build a typical boost converter circuit model in the Simulink as the fig. 1 shows.

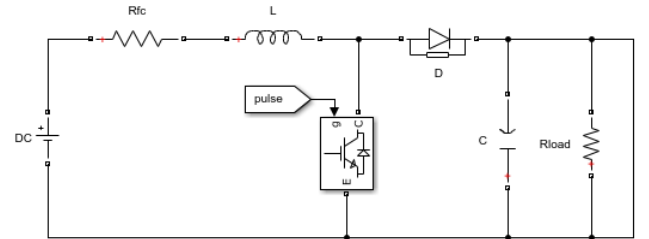


Fig 1. Simplified boost converter circuit

duty ratio of the switch could be given from (1) where V_i is the input voltage of the boost converter. And the DC source voltage from FC is defined as V_{FC} .

$$D = 1 - \frac{V_i}{V_o} = 1 - \frac{200}{480} = 0.5833 \quad (1)$$

Then the R_{load} as the output nominal of the boost converter could be given by

$$R_{load} = \frac{V_o^2}{P_{rated}} = \frac{480^2}{50000} = 4.608 \Omega \quad (2)$$

Therefore, the current flow through the inductor could be calculated from

$$I_L = \frac{V_d}{(1-D)^2 R} = \frac{200}{(1-0.5833)^2 * 4.608} = 250 A \quad (3)$$

Then, as for ripple of input current i_L , there is

$$\Delta i_L = \frac{V_s D}{L f} \quad (4)$$

where f is the switching frequency assumed as 100 kHz. The reason of selecting 100 kHz will be declared in section C. To meet the requirement that ripple of i_L is less than 20%

$$L \geq \frac{V_i D}{20\% I_L f} = \frac{200 \times 0.5833}{0.2 \times 250 \times 100000} = 2.332 \times 10^{-5} H \quad (5)$$

To minimize the ripple of input current, this study selected 0.55 mH for L . Additionally, the output voltage ripple is expected to be limited within 5%. From

$$\frac{\Delta V_o}{V_o} = \frac{D}{R_{load} C f} \leq 5\% \quad (6)$$

The value range of capacitor C could be given by

$$C \geq \frac{D}{5\% R_{load} f} = \frac{0.5833}{0.05 \times 4.608 \times 100000} = 25.317 \mu F \quad (7)$$

To minimize the output voltage ripple, this study selected 1.700 mF for C . All parameters evaluated in this section are shown in Table II.

TABLE II. PARAMETERS EVALUATED

Converter Parameters	Value
D	0.5833
L	0.55 mH
C	1700 μF
R_{load}	4.608 Ω
I_L	250 A

C. Switching Frequency and Switching Device Selection

Ripple current sets the scene for how much energy is stored by the inductor and given to the capacitor cyclically. At higher frequencies this transfer is done more times per second hence, for the same power delivered to a load, the ripple current could be smaller but this doesn't quite deliver the same power (energy proportional to current squared) and so the inductance has to be reduced and this increases the ripple current. The At low frequencies the inductor saturation is a big factor - lower the frequency and

saturation losses can suddenly skyrocket which causes bigger capacitor being required. In addition, switching frequency $f_{sw} \gg f_c$. While, exceedingly high frequency could products much switching losses due to

$$P_{sw} = \frac{1}{2} \frac{V_o I_o}{1-D} (t_r + t_f) f \quad (8)$$

To maintain the balance between dynamic and static losses in switching time, usually the switching frequency would not exceed 150 kHz. This study selected 100 kHz as switching frequency [3].

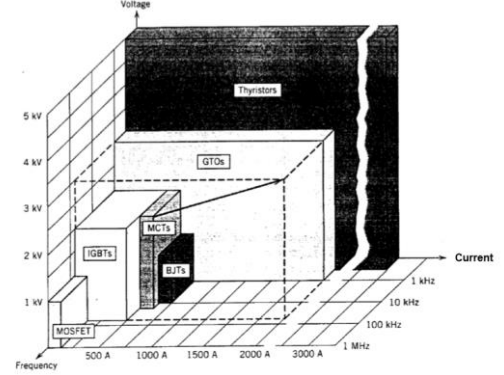


Fig 2. Summary of power semiconductor device capabilities

As shown in fig. 2, MOSFET is the best choice at 100 kHz switching frequency and a relatively low current burden. If select IRF540 as MOSFET switching device in this system, switch parameter $t_r = 50$ ns, $t_f = 20$ ns. The switching loss could be given by (8). As a result, P_{sw} is less than 1% P_o where P_o is the output power of the boost converter which equals the rated power.

III. MODELLING

This section builds up the dynamic modelling of designed boost converter to attain the transfer function of open loop system on which this study based to evaluate the stability of closed loop system.

A. State Space Averaging Modeling

This subsection derives the generalized equation for the continuous mode of the basic power converters. The continuous mode operation is simpler as there are only two states. The analysis starts from the state-space equations during the switch's on and off states shown as fig. 3 and uses an averaging method to linearize them. When the switching device is turned on, it conducts for a fraction D of a period.

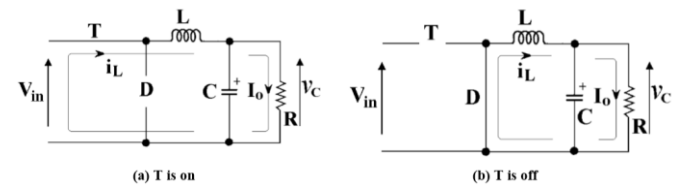


Fig 3. Two states of boost converter

To build the model, set up x , u , y first shown as equation (9)

$$\begin{cases} x = \begin{bmatrix} i_L \\ V_C \end{bmatrix} \\ u = [V_i] \\ y = [V_o] \end{cases} \quad (9)$$

From fig. 3

- When T is on:

$$\dot{x} = A_1 x + B_1 x \quad y = C_1 x \quad (10)$$

$$\begin{cases} \frac{dI_L}{dt} = \frac{V_i}{L} \\ \frac{dV_C}{dt} = -\frac{1}{RC} V_C \\ V_o = V_C \end{cases} \quad (11)$$

where R is R_{load} . From (9) (10) (11), could derive

$$A_1 = \begin{bmatrix} 0 & 0 \\ 0 & -\frac{1}{RC} \end{bmatrix} \quad B_1 = \begin{bmatrix} \frac{1}{L} \\ 0 \end{bmatrix} \quad C_1 = \begin{bmatrix} 0 \\ 1 \end{bmatrix} \quad (12)$$

- When T is off

$$\dot{x} = A_2 x + B_2 x \quad y = C_2 x \quad (13)$$

$$\begin{cases} \frac{dI_L}{dt} = -\frac{V_C}{L} + \frac{V_i}{L} \\ \frac{dV_C}{dt} = \frac{I_L}{C} - \frac{1}{RC} V_C \\ V_o = V_C \end{cases} \quad (14)$$

From (9) (12) (13), could get

$$A_2 = \begin{bmatrix} 0 & -\frac{1}{L} \\ \frac{1}{C} & -\frac{1}{RC} \end{bmatrix} \quad B_2 = \begin{bmatrix} \frac{1}{L} \\ 0 \end{bmatrix} \quad C_2 = \begin{bmatrix} 0 \\ 1 \end{bmatrix} \quad (15)$$

- Averaging

$$\dot{x} = Ax + Bx \quad y = Cx \quad (16)$$

$$\begin{aligned} A &= DA_1 + D'A_2 \\ B &= DB_1 + D'B_2 \\ C &= DC_1 + D'C_2 \end{aligned} \quad (17)$$

where

$$D' = 1 - D \quad (18)$$

- Small Signal

\hat{i}_L , \hat{V}_C , and \hat{d} are small-signal perturbations about the average DC or steady-state values of i_L , V_C and D respectively. After inputting small signal to original equations

$$\begin{cases} x = X + \hat{x} \\ u = U + \hat{u} \\ y = Y + \hat{y} \\ d = D + \hat{d} \end{cases} \quad (19)$$

Next, replace the variables in former equations by the (16) to generate DC items and small-signal items while eliminate the crossover small-signal items.

$$\begin{cases} A = DA_1 + D'A_2 = \begin{bmatrix} 0 & -\frac{D'}{L} \\ \frac{D'}{C} & -\frac{1}{RC} \end{bmatrix} \\ B = DB_1 + DB_2 = \begin{bmatrix} \frac{1}{L} \\ 0 \end{bmatrix} \\ C = DC_1 + D'C_2 = \begin{bmatrix} 0 \\ 1 \end{bmatrix} \\ E = (A_1 - A_2)X + (B_1 + B_2)U = \begin{bmatrix} \frac{V_C}{L} \\ -\frac{I_L}{C} \end{bmatrix} \end{cases} \quad (20)$$

$$\dot{\hat{x}} = A\hat{x} + B\hat{u} + E\hat{d} \quad (21)$$

$$\hat{y} = C\hat{x} \quad (22)$$

Deploy Laplace transformation to (18) (19) then get expected transfer function. When considering $\hat{d}(s) = 0$

$$\begin{aligned} G_{V_i}(s) &= \frac{\hat{y}(s)}{\hat{u}(s)} = \frac{\hat{V}_o(s)}{\hat{V}_i(s)} = C^T(sI - A)^{-1}B \\ &= \frac{1 - d}{CL \left(s^2 + \frac{1}{RC}s + \frac{(1-d)^2}{LC} \right)} \end{aligned} \quad (23)$$

When considering $\hat{V}_i(s) = 0$

$$\begin{aligned} G_{V_d}(s) &= \frac{\hat{y}(s)}{\hat{d}(s)} = \frac{\hat{V}_o(s)}{\hat{d}(s)} = C^T(sI - A)^{-1}E + (C_1 + C_2)X \\ &= \frac{V_o}{(1-d)} \frac{1 - \frac{sL}{(1-d)^2 R}}{1 + \frac{sL}{(1-d)^2 R} + \frac{s^2 LC}{(1-d)^2}} \end{aligned} \quad (24)$$

The expected transfer function of boost dc/dc converter could be derived as equation (22) by using state space averaging method.

B. Pulse Width Modular selection

This study chooses SG3525A as PWM which is a high-performance device with less external components. The peak value of sawtooth waveform V_m generated from this device is 2.4 V. So that the transfer function from amplified error to PMW section is

$$G_m(s) = \frac{\hat{d}(s)}{\hat{V}_C(s)} = \frac{1}{V_m} \quad (25)$$

C. System Stability Criterion

The stability is the ability that when perturbation disappears the system could return to the steady state. If the system cannot come back to the steady state, it is not a robust system. There are many criterions for system stability, this study selected Bode Plot to evaluate the system stability. a Bode plot is a graph of the frequency response of a system. It is usually a combination of a Bode magnitude plot, expressing the magnitude (usually in decibels) of the frequency response, and a Bode phase plot, expressing the phase shift [3].

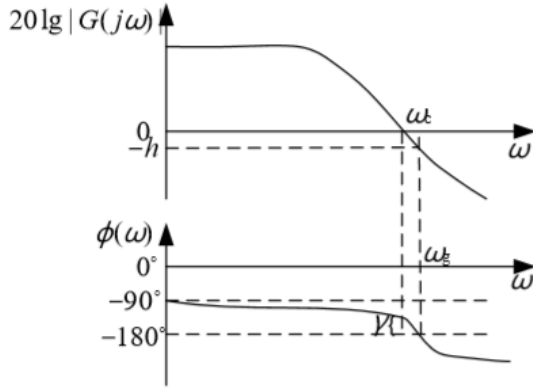


Fig 4. Bode Plot schematic diagram

Shown as fig. 4, the Bode Plot for a linear, time-invariant system with transfer function $G(s)$ consists of a magnitude plot and a phase plot.

- The Bode magnitude plot is the graph of the function $|G(j\omega)|$ of ω . A value for the magnitude $|G|$ is plotted on axis at $20 \log_{10} |H|$.
- The Bode phase plot is the graph of the phase, commonly expressed in degrees, of the transfer function $\arg G(j\omega)$ of frequency ω . The value for the magnitude $|G|$ is plotted on a linear vertical axis.

To ensure the robustness of system, the requirement of transfer function is that the Bode plot crosses the 0 dB line at a slop of -20 dB/dec(-1). Two concepts are introduced to value the stability of system.

1. Phase Margin

$$PM = 180^\circ + \phi\omega_c \quad (26)$$

where ω_c is the cross frequency when the $G(\omega_c)=1$.

2. Gain Margin

$$h = 20 \lg \frac{1}{|G(j\omega_g)|} \quad (27)$$

where ω_g is the frequency when $\phi(\omega_g) = (2k + 1)\pi, k = 0, \pm 1, \pm 2$.

Normally, to ensure the stability of system, PM is expected to be 30° to 60° , $h > 6$ dB and Bode magnitude plot should crossover 0 dB at a slop of -1.

D. Transfer Function Analysis with Bode Plot

For to design a satisfactory controller (compensator) including compensating network, this study selected Bode plot method to optimize the compensator. By utilizing the

conclusion from former sections, attain the Bode magnitude plot and phase plot and then improve the compensating network. While the open loop transfer function contains information influencing system stability and dynamic response. Hence, evaluating the open loop transfer function for system should be the first step of research and analysis.

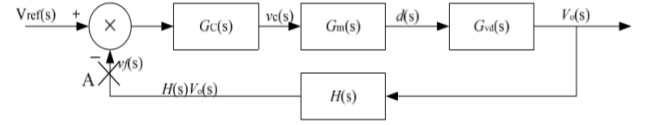


Fig 5. Block diagram of the control loop for the boost dc/dc converter.

From fig. 5, the transfer function of open loop system of boost converter could be written as

$$G(s) = G_c(s)G_m(s)G_{V_d}(s)H(s) \quad (28)$$

where $G_c(s)$ is the transfer function of compensator, and $H(s)$ is the transfer function of sample process.

$$H(s) = \frac{R_y}{R_x + R_y} \quad (29)$$

where R_y, R_x is the resistor in the sample circuit as shown in fig. 4.

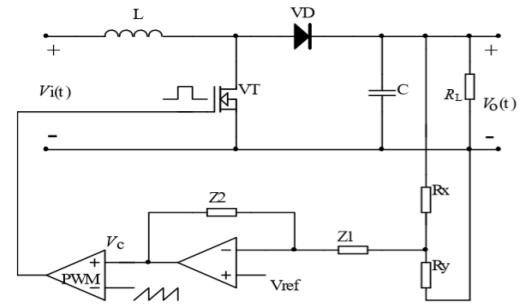


Fig 6. Boost converter control circuit diagram

Let $G_c(s) = 1$ to attain the open loop transfer function corresponding to system without the compensator [3].

$$\begin{aligned} G_1(s) &= G_{V_d}(s)G_m(s) \\ &= \frac{1}{V_m} \frac{V_o}{1-d} \frac{1 - \frac{sL}{(1-d)^2 R}}{1 + \frac{sL}{(1-d)^2 R} + \frac{s^2 LC}{(1-d)^2}} \\ &= \frac{480(1 - 6.875 \times 10^{-4} s)}{1 + 6.875 \times 10^{-4} s + 5.3856 \times 10^6 s^2} \quad (30) \end{aligned}$$

According to the equation above, code in Matlab to generate corresponding Bode plot shown as fig. 7.

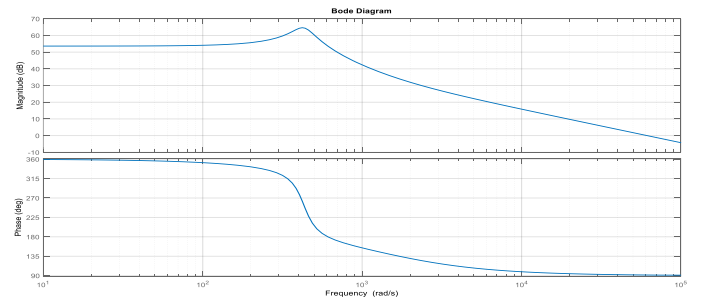


Fig 7. Boost converter without controller open loop system Bode plot

Key information could be attained from this Bode plot:

- The resonance existing in the system of which the magnitude is 64.6 dB.
- The transfer function crossover 0 dB line at a slope of -20 dB which is expected.
- Gain margin $h = 53.624 \text{ dB} > 0$ at $\omega_g = 609.4103 \text{ rad/s}$ which is satisfactory.
- Phase margin $PM = 88.5215^\circ$ at $\omega_c = 6.1304 \times 10^4 \text{ rad/s}$ which basically meets the requirements of robustness but not in the optimal range 30-60 degree.
- Conclusion: this system is basically stable.

IV. CONTROLLER DESIGN

A. Determine the parameters of PI Controller

Evaluating the parameters of the desired PI controller requires following the steps below [4].

1. Determine the Desired Crossover Frequency

Normally in the practical application, $f_c < \frac{1}{5} f_{sw}$ [3].

Then determine the desired crossover frequency ω_c , where the phase angle of plant $G_1(s)$ is $(180^\circ - \phi_m - \phi_c)$. ϕ_m is specified phase margin. ϕ_c is 5° normally which is the phase allowance for the angle contributed by the controller $G_c(s)$ at ω_c . If select desired phase margin as 60° . From $G_1(s)$ Bode plot, select the desire $\omega_c = 3.43 \times 10^3 \text{ rad/s}$ where the phase angle of $G_1(s)$ is 115°

2. Determine K_p

Determine K_p that $K_p G_1(s)$ crosses the 0-dB axis at the specified ω_c . Assuming that $K_p = 0.0507$, that $K_p G_1(s)$ crosses the 0-dB axis at $\omega_c = 3.43 \times 10^3 \text{ rad/s}$ shown as fig.8.

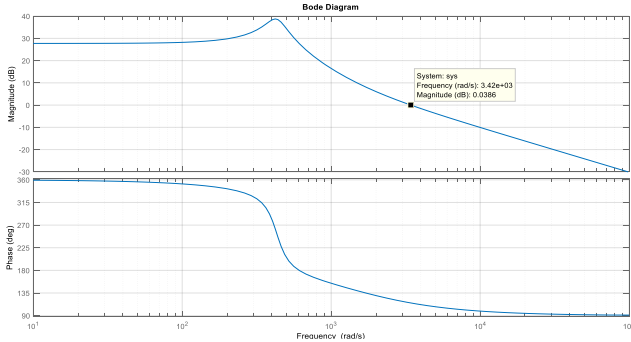


Fig 8. $K_p G_1(s)$ Bode plot

3. Determine K_i

Choosing the break frequency K_i/K_p of rh controller one decade below ω_c , that is, $K_i/K_p = \omega_c/10$. So this study selected $K_i = 3430 \div 10 \times 0.0507 = 17.3901$. Hence the transfer function of controller is

$$G_c(s) = K_p + \frac{K_i}{s} = \frac{0.0507s + 17.3901}{s} \quad (31)$$

B. Bode Plot of Boost Converter with PI Controller

Plot the $G_c(s)G_m(s)G_{V_d}(s)$

$$\begin{aligned} G_2(s) &= G_c(s)G_m(s)G_{V_d}(s) \\ &= \frac{0.0507s + 17.3901}{s} \frac{480(1 - 6.875 \times 10^{-4}s)}{1 + 6.875 \times 10^{-4}s + 5.3856 \times 10^6 s^2} \\ &= \frac{-0.016731s^2 + 18.5973s + 8347.248}{5385600s^3 + 6.875 \times 10^{-4}s^2 + s} \end{aligned} \quad (32)$$

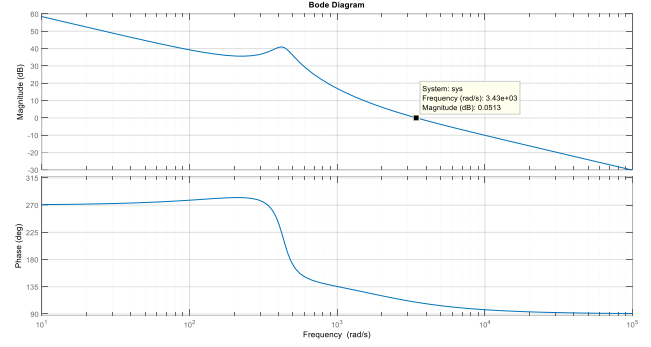


Fig 9. Boost converter with controller open loop system Bode plot

From fig.9. the Bode plot of the boost converter with controller open loop system, the following information could be attained.

- The transfer function crossover 0 dB line at a slope of -20 dB which is expected.
- Gain margin $h = 37.7266 \text{ dB} > 0$ at $\omega_g = 480.1849 \text{ rad/s}$ which is satisfactory.
- Phase margin $PM = 70.628^\circ$ at $\omega_c = 3.4412 \times 10^3 \text{ rad/s}$ which basically meets the requirements of robustness closer to optimal range 30-60 degree than the system without the controller.
- Conclusion: this system is basically stable.

C. Compensating Network Topology

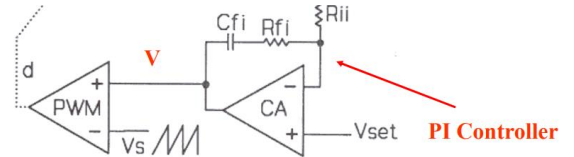


Fig 10. PI controller topology

The diagram of the boost converter with PI controller is shown as fig.10.

$$G_c(s) = \frac{\frac{R_{fi}}{R_{ii}}s + \frac{1}{R_{ii}C_{fi}}}{s} \quad (33)$$

Assuming $R_{ii} = 10 \text{ k}\Omega$, so $R_{fi} = 0.0507R_{ii} = 507\Omega$,

$$C_{fi} = \frac{1}{17.3901 \times 10000} = 5.75 \mu\text{F}.$$

V. SIMULATION

Built the complete boost converter model in the Simulink as shown in fig.11.

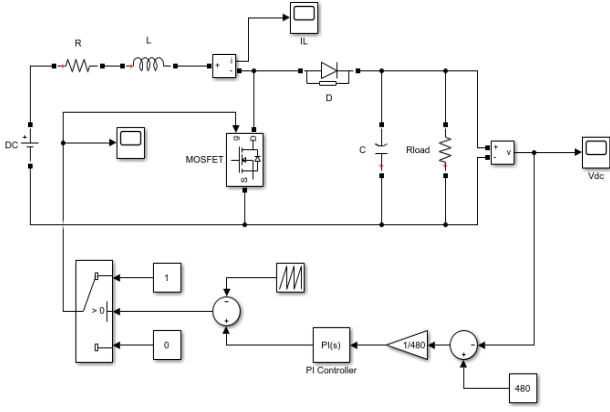


Fig 11. Boost converter with PI controller model

In this model, the $H(s)$ is set to $1/480$ (480 V being the desired voltage at the dc bus) to normalize the output dc voltage presented in the gain block of the Simulink model. All parameters are set as former equations product. The results and analysis of the simulation are as follow.

1. Output Voltage V_o

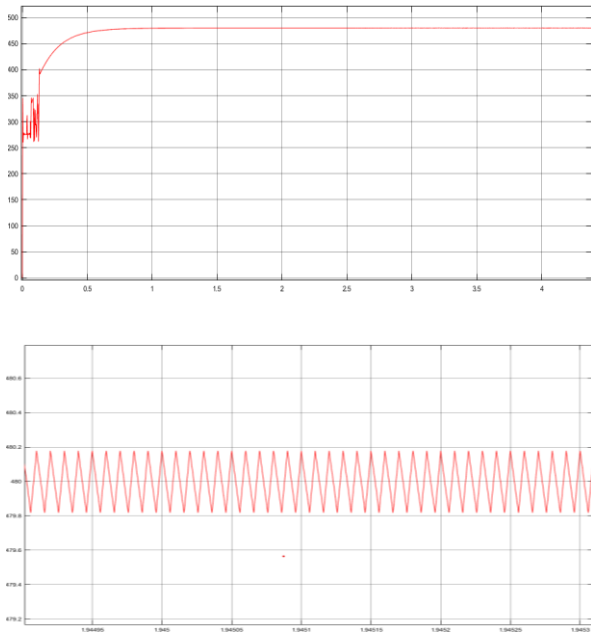


Fig 12. The output voltage

As fig.12 shows, the output voltage is steady at 480 V and the ripple is limited within 0.4 V, that $\frac{\Delta V_o}{V_o} < \frac{0.4}{480} = 0.08\% < 5\%$ which meets the design requirement.

2. Input Current I_L

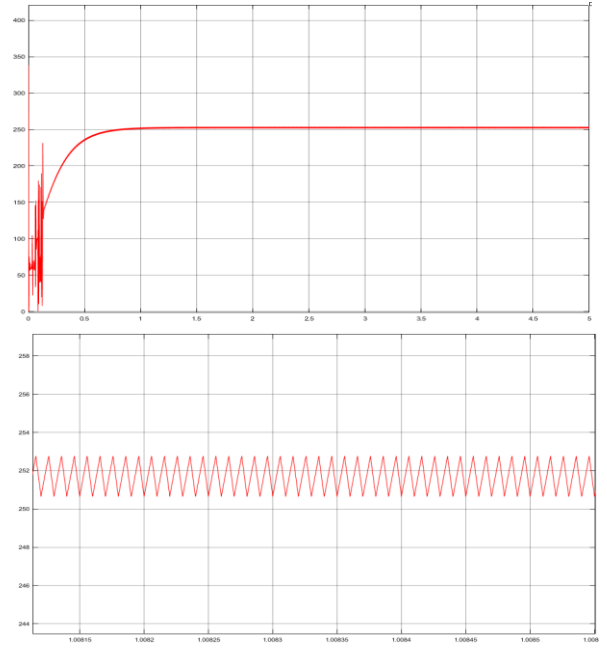


Fig 13. The input current ripple

As fig.13 shows, the input current is steady at around 251V and the ripple is limited within 3 V, that $\frac{\Delta I_L}{I_L} < \frac{3}{250} = 1.2\% < 20\%$ which meets the design requirement.

3. Pulse Width

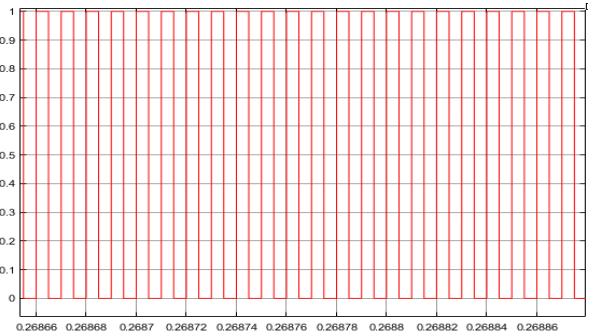


Fig 14. The pulse width

The width of the pulse modulated by PMW and PI controller is close to the desired width providing fairly accurate duty ratio which has an expected value of 0.5833.

VI. CONTROLLER DESIGN

A dc/dc boost converter with PI controller for a 50-kW Proton Exchange Membrane Fuel Cell (PEMFC) stack is designed to regulate the output voltage of the fuel cell stack from 300 V to 480 V meanwhile meeting the requirement that the input voltage of the boost converter should be 200 V. This study designed the fundamental boost converter circuit in the section II including the determination of necessary electrical components. While in the section III, the dynamic model of

the power stage with output filter was built and the PWM is desinged to obtain the transfer function of open loop system without the controller. Additionally, also the criterions for system stability was introduced and then stability analysis using Bode plot for the system was completed. The PI controller is designed deploying the combination of Bode Plot and compensating network topology in section IV. Finally the simulation was completed in section V in which all design requirments given in Table. I are all satisfied by output voltage and input current plots.

VII. COMPONENTS SELECTION TABLE

TABLE III. COMPONENTS SELECTION

Component Name	Product Name
Pulse Width Modular MOESFET	SG3525A IRF540
Diode	MBR20100CT
0.55mH Inductor	UCC28180
1700 μ F Capacitor	CGH172T250V2L

REFERENCES

- [1] M. Forouzesh, "Step-up dc-dc converter: a comprehensive review of voltage-boosting techniques, topologies and techniques," IEEE Trans. Power Electron., vol. 32, no. 12, pp. 9143, Dec 2017.
- [2] K. J. Reddy, "High voltage gain interleave boost converter with neural network based MPPT controller for fuel cell based electric vehicle," IEEE Access, Feb 2018.
- [3] J. Guo, "Voltage-control model boost converter system analysis and design," Master's thesis, 2010.
- [4] C. Wang, M.H. Nehrir, and S.R. Shaw, "Dynamic models and model validation for PEM fuel cell using electrical circuits," IEEE Trans. Energy Conversion, vol. 20, no. 2, pp. 442-451, Jun 2005.